DELPHI Collaboration

DELPHI 2002-046 CONF 580
10 June, 2002

Search for single top quark production in the framework of R-parity violation

V. Poireau

CERN, CH-1211 Geneva 23, Switzerland

Abstract

A search for a signal $e^+e^- \longrightarrow t\bar{c}/t\bar{u}$ in the framework of supersymmetry with R-parity violation is presented. The data collected by the DELPHI detector at centre-of-mass energies from 189 GeV to 209 GeV (with an integrated luminosity of 608 pb^{-1}) have been analysed. Both the hadronic and semi-leptonic channels were studied. No evidence for a signal was found in any of these channels. The results were combined to provide an upper limit on the production cross-section of these signals, as well as a direct limit on the λ' coupling constants involved in these processes.

Contributed Paper for ICHEP 2002 (Amsterdam)

1   Introduction

1.1   R-parity violation

The most general superpotential of the minimal supersymmetric standard model (MSSM) can be expressed in a sum of two terms:

$$W_{MSSM} = W_{R_p} + W_{\not{R}_p},$$

where W_{R_p} is the classical term of the MSSM [1] and where $W_{\not{R}_p}$ reads[1]:

$$W_{\not{R}_p} = \lambda_{ijk} L_i L_j E_k^c + \lambda'_{ijk} L_i Q_j D_k^c + \lambda''_{ijk} U_i^c D_j^c D_k^c.$$

The numbers i, j and k are the generation indices; L and E represent respectively the left-handed doublet and the right-handed singlet of the lepton superfield; Q, U and D denote respectively the left-handed doublet, the up-type right-handed singlet and the down-type right-handed singlet of the quark superfields; λ_{ijk}, λ'_{ijk} and λ''_{ijk} are Yukawa couplings. We consider here models where we keep the $W_{\not{R}_p}$ term in the superpotential. This term violates the R-parity quantum number, defined as $R_p = (-1)^{3B+L+2S}$ (B being the baryonic number, L the leptonic number and S the spin of the particle).

At the phenomenological level, the main consequence is that the lightest supersymmetric particle (LSP) can decay into standard particles and therefore may be visible within the detector volume. In addition, one single superparticle can be produced in the collision of two standard particles.

1.2   Data sample and experimental apparatus

The data used in this analysis were collected by the DELPHI detector in 1998, 1999 and 2000. In 1998, 158 pb^{-1} were collected at an energy in the centre-of-mass equal to 189 GeV. In 1999, the energy was varying between 192 GeV and 202 GeV with a total luminosity of 226 pb^{-1}. In 2000, the energy in the centre-of-mass was contained between 200 GeV and 209 GeV with a total luminosity of 224 pb^{-1}. The DELPHI apparatus is described in detail in [2].

2   Single top quark production

2.1   Production

The product of coupling constants $\lambda'\lambda''$ is strongly constrained by the lower limit on the proton lifetime. Thus, to avoid a proton decay, we assume here that the λ' couplings are dominant (i.e. λ and λ'' couplings are negligible or equal to zero).

The λ' couplings imply an interaction between one slepton and two quarks, or between one squark, one quark and one lepton. At LEP, theses interactions can occur at the production level. An experimentally interesting possibility, which is studied in this paper, is shown in figure 1. In this diagram, a down-type squark (i.e. the supersymmetric partner of the down-type quarks d, s or b) is exchanged in the u-channel. The final state, before decay, is composed of a t quark together with a c or u quark. Two different λ'_{ijk} coupling

---

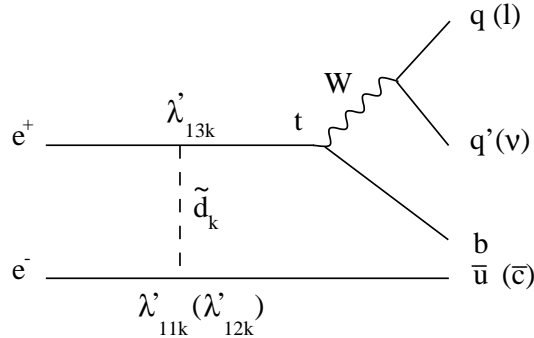[1]We made here the assumption that the term $\mu'_i H_2 L_i$ of the superpotential could be rotated away.

Figure 1: Production and decay of the $t\bar{u}$ (respectively $t\bar{c}$) final state at LEP via the coupling constants λ'_{13k} and λ'_{11k} (respectively λ'_{12k}). The generic notation $\tilde{d}$ for the exchanged squark denotes the three down-type squarks $\tilde{d}$, $\tilde{s}$ and $\tilde{b}$.

constants are involved in this diagram. The vertex with the positron and the t quark implies a λ'_{13k} coupling: the first index represents the electron family ($i = 1$), the second one represents the t quark family ($j = 3$) and the third index stands for the down-type squark family (with $\tilde{d}_1 \equiv \tilde{d}$, $\tilde{d}_2 \equiv \tilde{s}$ and $\tilde{d}_3 \equiv \tilde{b}$ - no assumption is made on the value of the k index). The second coupling constant corresponds to λ'_{12k} for a c quark in the final state, and to λ'_{11k} for a u quark.

Due to its large mass ($m_t = 174.3 \pm 5.1$ GeV/c^2), the lifetime of the t quark is very short: 4×10^{-25} s. Consequently, the t quark decays before QCD effects take place: $t \longrightarrow bW$ (with a branching ratio close to 100%)[2]. This decay constitutes a clean signature at LEP. A mass reconstruction is possible for the W boson and for the t quark, as well as an extensive use of the b-tag.

In this paper, both the hadronic and semi-leptonic channels were studied:

$$
\begin{aligned}
e^+e^- &\longrightarrow t\bar{c}(\bar{u}) \longrightarrow qq'\, b\bar{c}(\bar{u}); \\
e^+e^- &\longrightarrow t\bar{c}(\bar{u}) \longrightarrow l\nu\, b\bar{c}(\bar{u}).
\end{aligned}
$$

Although this study was already proposed [3, 4, 5], this signal was never searched for at LEP in the framework of R-parity violation. Nonetheless, this signal was studied in other models in DELPHI [6].

The fact that the coupling constants are involved in the production allows a direct evaluation of their strength (from the knowledge of the production cross-section). If no signal is discovered, limits would be derived on the product of the two coupling constants. These limits are called *direct limits*, as in this study we will probe directly the values of the couplings. Most constraints on the R-parity violating couplings come from precision measurements: these *indirect limits* are computed from the difference between these measurements and the theoretical prediction in the standard model. These two kinds of approach are complementary.

---

[2]We assume here that the superparticles are too heavy to give a contribution to this decay. The D0 collaboration set a limit at 252 GeV/c^2 on the squarks after an analysis with a dominant λ' coupling. This limit is dependent on some assumptions, but has justified the restriction on the t quark decay in standard particles.

2.2 Motivations

In the standard model, because of the unitarity of the Cabbibo-Kobayashi-Maskawa (CKM) matrix, these processes are strictly forbidden at the tree level. Furthermore, they are strongly suppressed at the loop level due to the Glashow-Iliopoulos-Maiani (GIM) mechanism [7]. In the standard model, the cross-section of the process $e^+e^- \longrightarrow t\bar{c}$ is around 10^{-9} fb at 200 GeV [8]. LEP would have to run during several billion years to hope to see one event with a t quark and a c quark. A discovery of such events would sign without ambiguity a process resulting from physics beyond the standard model.

The contributions of the MSSM with R-parity conservation come from mixture of squarks. However, it was shown that the process $e^+e^- \longrightarrow t\bar{c}$ gave negligible contributions not observable in a detector [9]. It is also possible to study this process in the framework of a general model with two Higgs doublets. The results show that the number of expected events is too low to be measurable at LEP [10].

The next subsection presents the predicted cross-section in the framework of R-parity violation.

2.3 Cross-section

The computation of the theoretical cross-section was done in the references [3, 4], and reads:

$$\frac{d\sigma}{dt} = \frac{N_c}{16\pi s^2} \sum_k \frac{u(u - m_t^2)}{(u - m_{\widetilde{d}_k}^2)^2} |\lambda'_{1jk} \lambda'^*_{13k}|^2, \tag{1}$$

with $N_c = 3$, $t = -\frac{1}{2}(s - m_t^2)(1 + \cos\theta)$, $u = -\frac{1}{2}(s - m_t^2)(1 - \cos\theta)$, θ being the angle between the positron and the t quark and $\sqrt{s}$ the centre-of-mass energy. The $m_{\widetilde{d}_k}$ quantity represents the mass of the down-type squark. The j index is equal to 1 for $e^+e^- \longrightarrow t\bar{u}$ and to 2 for $e^+e^- \longrightarrow t\bar{c}$.

The integration of this formulae on the θ angle gives:

$$\sigma = \frac{N_c}{32\pi s^2} \sum_k |\lambda'_{1jk} \lambda'^*_{13k}|^2 \left[(s - 2m_t^2) + \frac{m_{\widetilde{d}_k}^2 s}{s + m_{\widetilde{d}_k}^2 - m_t^2} \right.$$
$$\left. -(2m_{\widetilde{d}_k}^2 - m_t^2) \ln \frac{s + m_{\widetilde{d}}^2 - m_t^2}{m_{\widetilde{d}_k}^2} \right]. \tag{2}$$

This expression corresponds to the production cross-section of the $t\bar{u} + \bar{t}u$ (for $j = 1$) and the $t\bar{c} + \bar{t}c$ (for $j = 2$) final states. This cross-section depends on the collision energy, on the value of the coupling constants and on the exchanged squark mass. In the following, we suppose that only one type of squark is light enough to be involved in the production diagram: consequently, the summation on the k index disappears. This hypothesis avoids overestimation of the production rate of the events.

To simplify the event generation (see next section), only a squark mass of 100 GeV/c^2 was implemented in the simulation of the process $e^+e^- \longrightarrow t\bar{c}$. Using the $d\sigma/d\theta$ expression, we can show that there is only a small influence of the squark mass on the angular distribution as soon as its mass is contained between 70 and 1000 GeV/c^2. The analyses done at LEP under the assumption that a λ' coupling dominates give a limit of 74 GeV/c^2 on the lighter squark [11]. Furthermore, a squark mass greater than 1000 GeV/c^2 is not

favoured by naturalness arguments. Thus, the presented analyses will not be sensitive to the generated squark mass.

2.4 Generation

A generator was specially written for the analysis presented in this paper [12]. The reaction $e^+e^- \longrightarrow t\bar{c}$ was generated in the u channel with the differential cross-section (1). A mass of 100 GeV/c^2 was chosen for the squark, and the t mass was equal to 173.8 GeV/c^2. The initial state radiation was taken into account and implemented into the generator. JETSET took charge of the decays of the t quark and of the W boson and hadronisation was performed by the generator. The correction on the gluon splitting was also taken into account in order to have the best value of the b-tagging in the Monte-Carlo simulations. After this generation, the standard DELPHI program for the detector simulation, DELSIM [13], and the standard DELPHI program for the reconstruction, DELANA [14], were used.

The simulation of the $t\bar{c}$ process was performed for the 1998, 1999 and 2000 data. The signal was simulated with a centre-of-mass energy of 189 GeV in 1998, of 200 GeV in 1999 and of 206 GeV in 2000. It was assumed that the efficiency changed only slightly for 1999 and 2000 where several centre-of-mass energies were delivered by LEP. For each sample, 2000 events were generated.

Notice that only the final state with a c quark was generated. In the following, we will only mention the $t\bar{c}$ signal, but the study will be applicable for a u quark. Effectively, these two quarks are very light, and no difference is expected in the kinematics.

Moreover, the generation is only valid for an exchanged squark of the first or of the second generation. For the third family, the mixing between squarks can be important so that the cross-section is modified. This effect was not implemented in the generator: thus the search will be only valid for the coupling constants λ'_{11k}, λ'_{12k} and λ'_{13k} with $k = \{1; 2\}$.

2.5 Kinematics

The kinematics of the $t\bar{c}$ helps for the discrimination against the standard model processes. For a centre-of-mass energy of 189 GeV, the c quark energy is equal to 13.5 GeV, for 200 GeV, it is equal to 23.5 GeV and for 206 GeV, it is equal to 28.5 GeV. Moreover, if the energy in the centre-of-mass frame is close to the threshold for the $t\bar{c}$ production, the energy of the b quark is closed to 69 GeV.

3 Indirect limits on the product of coupling constants

In this section, we present the indirect limits determined on the product of the coupling constants studied in this paper. The method consists to study processes for which there is a possible contribution coming from the R-parity violation. The non-observation of deviations is used to set limits on the couplings.

The study of the reaction $B \longrightarrow X\nu\bar{\nu}$ was employed to put constraints on the product of couplings. This reaction is allowed in the standard model via box and penguin diagrams. The computation shows that the branching ratio (Br) of this decay is equal to: $\text{Br}(B \longrightarrow$

$X\nu\bar{\nu}) = (3.5 \pm 0.7) \times 10^{-5}$. This final state was searched for by the ALEPH collaboration in the LEPI data [15]. The limit they obtained on this process was found to be (at the 90% of confidence level): $\mathrm{Br}(B \longrightarrow X\nu\bar{\nu}) < 7.7 \times 10^{-4}$. The contribution from the R-parity violation at the $B \longrightarrow X\nu\bar{\nu}$ process involves a down-type squark. The limit given by ALEPH leads to the following constraints on the couplings related to the interaction (at the 95% of confidence level) [16]:

$$\lambda'_{ijk}\lambda'_{i'3k} < 1.8 \times 10^{-3} \left(\frac{m_{\widetilde{d}_k}}{100 \ \mathrm{GeV}/c^2} \right)^2. \tag{3}$$

These limits are very stringent. The present search will not be able to give a better limit with respect to (3). However, the constraints given above result from a comparison between the prediction of the standard model and supersymmetry with R-parity violation. These comparisons depend on a large number of factors and approximations, on difficult computations at the loop level, on uncertainties (as the t quark mass or as the CKM matrix elements), as well as on the spectrum of supersymmetric particles. In this paper, we propose to present a *direct search* for a process predicted by supersymmetry with R-parity violation. The interpretation of this search will be straightforward and will lead in a simple way to an evaluation (measure or limit) of the coupling constants. The results of this paper will be complementary of the results shown above.

4 Search in the hadronic channel

4.1 Preselection

The preselection was mainly based on the number of charged tracks, on the visible and charged energy, on the thrust and on transition values given by the jet algorithm (see below for the choice of the jet algorithm).

After this preselection, for the 2000 analysis, 1856 events were seen in the data, to be compared with 1850 events expected with the Monte-Carlo simulation (in 1999: 2196 compared to 2110; in 1998: 1118 compared to 1118). At this stage of the analysis, only the 4 fermion backgrounds (W^+W^- and ZZ) and the $q\bar{q}$ background remained. The total signal efficiency was around 50% for the 3 years (total means that all channels, hadronic and semi-leptonic, were taken into account in the efficiency).

4.2 Identification of jets

First of all, the events were forced into 4 jets. The chosen algorithm was the Cambridge algorithm [18]. This algorithm improved the analysis performances. Effectively, the c quark energy being low, the use of this algorithm, thanks to the *soft freezing*, prevents c jet to attract particles not belonging to it: the energy of the c quark was better estimated. A comparison was performed at 189 GeV between the Cambridge algorithm and the Durham algorithm: an improvement of 7% in determining the c quark energy was observed with the use of the Cambridge algorithm.

In order to reconstruct the masses of the t quark and of the W boson, the 4 jets of the event have to be identified with the quarks q, q', b and c (see figure 1). The chosen method was identical for all studied energies (from 189 GeV to 209 GeV). The procedure was the following:

- the event was forced into 4 jets with the Cambridge algorithm;
- a 4 constraint kinematical fit was performed on the jets;
- the c jet was defined as the less energetic jet;
- amongst the remaining jets, the b jet was defined as the one which had the highest value of b-tag;
- the 2 remaining jets were considered coming from the W.

This procedure used no mass informations (as for example the t or W mass), which allowed to keep the discriminant power of these variables. Moreover, the c jet can have a non negligible b-tag, but this property was not taken into account since the analysis had to be valid without changes to the case of the $t\bar{u}$ signal.

4.3 Mass reconstruction

As soon as the identification of the jets is performed, it is straightforward to reconstruct the masses of the event. The energies and the momenta determined with the kinematical fit were used to compute the invariant masses. Figure 2 presents the mass reconstruction for the t quark and for the W boson for 203-209 GeV.
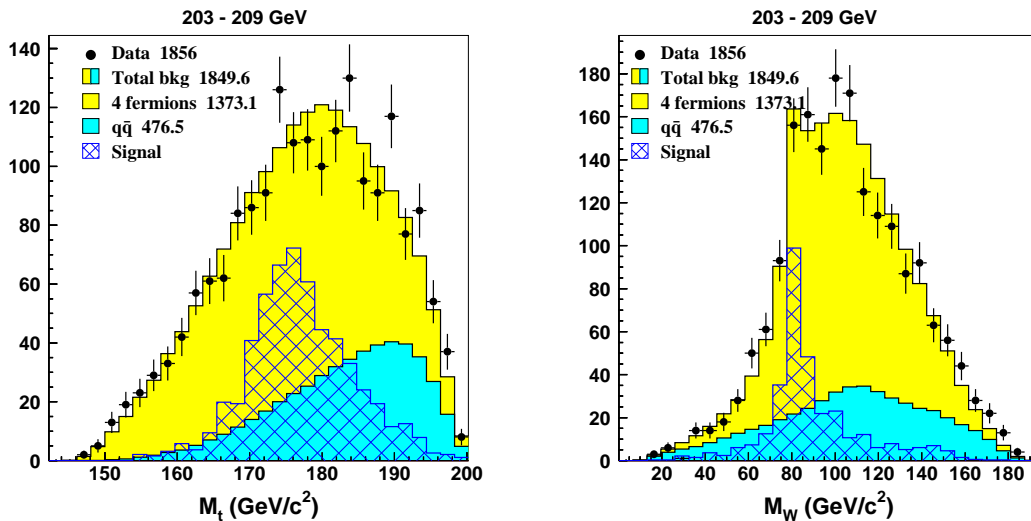

Figure 2: Left plot: invariant mass of the 3 jets coming from the t quark candidate at 203-209 GeV. Right plot: invariant masses of the two jets coming from the W candidate at 203-209 GeV. The signal corresponds to the hatched histogram (with an arbitrary normalisation).

The resolutions on the t quark mass for the signal are indicated in table 1 for the 3 years studied in this paper. We observe that the resolution is lower for higher energies. This is explained by the quality of the fit which decreases when the phase space expands (i.e. when the collision energy is increasing).

4.4 Choice of the discriminant variables

The following variables were used in the analysis:

Energy (GeV)	189	200	206
Resolution (GeV/c^2)	4.1 ± 0.1	6.3 ± 0.2	7.2 ± 0.2

Table 1: Resolutions on the reconstructed mass of the t quark candidate for a signal simulated at 189, 200 and 206 GeV (hadronic channel).

- the energy of the c jet candidate (after a 4 constraint fit);
- the reconstructed mass of the W candidate (after a 4 constraint fit);
- the value of the χ^2 coming from a 6 constraint fit performed on the chosen combination (and only on this combination). The two additional constraints corresponded to the t mass and to the W mass.
- the b-tag of the b jet candidate;
- the sum of the b-tag of the jets from the W candidate (which was used as an anti-b-tag variable);
- the thrust;
- $\alpha_{min} \times E_{min}$ after having forced the event into 4 jets (α_{min} is the minimum angle amongst the jets and E_{min} is the energy of the less energetic jet);
- $\alpha_{min} \times E_{min}$ after having forced the event into 5 jets;
- $-\log_{10}(y_{32})$, the transition value which makes the event flips from 3 to 2 jets;
- $-\log_{10}(y_{43})$, the transition value which makes the event flips from 4 to 3 jets;

The t quark mass was not used since this variable was strictly correlated with the energy of the c quark.

4.5 Neural net

These 10 discriminant variables were set as inputs of a neural network (using the package MLPFIT [19]). This network was composed of 1 input layer with as many neurons as the number of discriminant variables, 1 hidden layer with the same number of neurons as the input layer and 1 output layer with 1 neuron. Signal events as well as background events were presented to the network for the training step. Due to a low number of simulated signal events, theses events were not divided into two samples for the training. However, it was checked that 100 epochs of learning allowed to avoid overtraining. Following this stage, the real data and the different background events were presented to the network. This network gives an answer (the value of the output neuron) which is an approximation of the probability that an event is signal-like. A cut step by step was performed on the output value. As an example, the result is shown for the 203-209 energies in figure 3.

For all energies, a good agreement between collected data and expectations from the standard model was observed. This agreement shows that no signal was seen in the data and therefore the cut could be optimised in order to increase the exclusion power. The working point corresponded to the cut which allowed to reach the minimum of the expected limit on the excluded cross-section.

4.6 Results

The choices of the working points for the three years lead to the results presented in table 2. The quoted efficiencies correspond to the total signal sample (i.e. hadronic and

semi-leptonic channel).

The efficiencies shown in the table are also valid for a $t\bar{u}$ signal. It was checked that the "*b-tag*" of the c quark played no role in the selection of events. In particular, when there was a mistake in the jet identification, the analysis showed that the inversion concerned the b jet and one of the jets from the W: thus the c jet was not involved by mistake in the evaluation of the b-tag.

	Data	Standard processes	4 fermions	$q\bar{q}$	ε_{signal} (%)
1998	11	12.4 ± 0.47	4.0 ± 0.20	8.4 ± 0.41	19.7 ± 0.88
1999	11	11.4 ± 0.42	4.6 ± 0.18	6.8 ± 0.38	16.4 ± 0.82
2000	20	21.2 ± 0.29	11.7 ± 0.22	9.5 ± 0.20	18.9 ± 0.88

Table 2: Number of selected events after the cut on the output value of the neural network for the data and for the different standard processes. The last column represents the total efficiency for a signal $e^+e^- \longrightarrow t\bar{c}$. The results are shown for the years 1998 to 2000. The quoted errors are only statistical.

5 Search in the semi-leptonic channel

5.1 Preselection

The general characteristics of a signal $e^+e^- \longrightarrow l\nu\, b\bar{c}$, used to perform the preselection, are the following:

- the event has to contain either an energetic electron or muon, either a tau jet with a small multiplicity;
- the lepton is isolated with respect to the other tracks;
- a missing energy is expected due to the neutrino(s);
- nonetheless, presence of jets leads to a large visible energy.

The algorithm used for the identification of leptons was provided by the W DELPHI team [17]. The tracks associated with the identified lepton were removed and the rest of the event was forced into two jets.

The results of the identification of the leptons were the following: at the end of the preselection, 61% of the electrons of the signal were identified as electrons by the algorithm, 74% of the muons were identified as muons and 49% of the taus were identified as taus.

The composition of the background depended on the lepton. The main background was constituted of 4 fermion processes. Especially in the case of taus, it remained some events $e^+e^- \longrightarrow q\bar{q}(\gamma)$. There was also a small proportion of 2 photon processes ($e^+e^- \xrightarrow{\gamma\gamma} e^+e^- X$ where X stands for a hadronic or leptonic state).

For the 2000 analysis, the results after the preselection were, for the electron channel, 375 events seen in the data for 410 expected in the framework of the standard model; for the muon channel, 373 observed events for 390 expected events; for the tau channel, 275 observed events for 246 expected events. The total efficiency for the $t\bar{c}$ signal (for the 2000 analysis) was equal to 6.6% for the electron channel, 8.1% for the muon channel and

5.3% for the tau channel, leading to a cumulated efficiency for the three leptons equal to 20%.

5.2   Mass reconstruction

The semi-leptonic channel contains less ambiguities compared to the hadronic one. The particles produced in the reaction are various and made the reconstruction easier.

The first step consisted of computing the energy and the momentum of the neutrino: these values were simply determined thanks to the missing energy and to the missing momentum. Then a kinematical fit with one constraint was applied on the quadri-vector energy-momentum of the quarks, of the charged lepton and of the neutrino. This fit gave the energies and the momenta of these particles.

For the signal, the energy of the c quark is always lower than the energy of the b quark. Thus, the jet coming from the c quark was defined as the less energetic jet[3].

The resolution on the reconstructed mass of the t quark is presented for the signal in table 3. These results can be compared with those in the hadronic channel (table 1). The resolutions have the same magnitude. The hadronic channel involves no missing energy, but the uncertainty on the jet association to form the t quark decreases the resolution. In the semi-leptonic channel, the particle association is easier but the resolution is reduced by the presence of the neutrino.

	Energy (GeV)	189	200	206
Electron channel	Resolution (GeV/c^2)	4.5 ± 0.3	6.4 ± 0.7	7.1 ± 0.8
Muon channel	Resolution (GeV/c^2)	3.8 ± 0.3	6.6 ± 0.6	8.8 ± 0.8
Tau channel	Resolution (GeV/c^2)	6.9 ± 1.2	6.5 ± 0.8	9.9 ± 1.3

Table 3: Resolution on the reconstructed mass of the t quark for a signal simulated at 189, 200 and 206 GeV for the three semi-leptonic channels.

5.3   Choice of the discriminant variables

One separate analysis for each type of lepton was performed. Effectively, the background composition depends on the lepton which is studied, and it is therefore preferable to train three separate neural networks. The characteristics of each type of lepton is then better taken into account and the analysis, after the combination of the results, is improved.

The analysis in the muon channel will present the best results: the precise measurement of the energy and momentum of the muon allows a good discrimination. Furthermore, we have seen that the reconstruction efficiency was better for this lepton (74% of real muons are identified as muons by the identification algorithm). Therefore a small number of discriminant variables was useful to train the neural network. The electron channel presents slightly lower performances with respect to the muon channel. Concerning the tau channel, the analysis will suffer from a weaker power of discrimination, which can be explained first because the determination of the energy and of the momentum is

---

[3]The method for the jet identification did not used the value of the b-tag since the c jet could have sometimes a higher value of the b-tag than the b jet.

difficult and second because the efficiency of reconstruction is only equal to 49%. To compensate for this effect, the neural network has to contain more informations to increase the discrimination power, and will therefore be composed of a higher number of variables.

Variables based on kinematics: the c quark energy as well as the b quark energy were used to distinguish the signal from the processes of the standard model. The W reconstructed mass was also involved in the analysis. Moreover, the main background was composed of events $W^+W^- \longrightarrow qq'l\nu$: in this case, the invariant mass of the two quarks was equal to the W mass (which was not true for the signal), and justify the use of this variable in the analysis. Finally, the missing transverse momentum was also used, and allowed to discriminate against the $q\bar{q}(\gamma)$ events.

Variable based on b-tag: the signal events contain one b quark whereas the main background (W^+W^-) does not contain such type of quarks. Thus the b-tag of the b jet candidate was included in the analysis.

Variables characterising the event topology: the transition values $-\log_{10}(y_{21})$ and $-\log_{10}(y_{32})$ were employed to help for the discrimination. These values were computed after having removed the lepton tracks. For the electron and tau channel, the quantity $\sqrt{s'}$ was also involved in the analysis.

Variables used only in the tau channel: as it was said, additional variables were needed to improve the analysis in the tau channel. Firstly, the tau energy was included in the training of the neural network. Furthermore, a 5 constraint fit was applied on the event: equality was imposed between the invariant mass of jets and the invariant mass of the tau and its neutrino. This fit was perfectly adapted to the W^+W^- process and led to a precise mass reconstruction of the W. For the signal, this mass took arbitrary values. A 6 constraint fit was performed on the jets and leptons of the event. The two additional constraints imposed the W mass on the invariant mass of the tau and the neutrino, and the t mass on the invariant mass on the tau, the neutrino and the b jet candidate. This fit produced a χ^2 value lower for the signal than for the other backgrounds. Several angles were used for the discrimination. First of all, the cosine of the angle between the beam direction and the missing momentum, as well as the cosine of the isolation angle, were introduced in the neural network. In addition, the cosine of the flight angle of the W boson (for the signal) was computed: the distribution was flat for the signal whereas the variable took values close to 1 for $q\bar{q}$ events. The cosine of the angle of the tau in the W boson frame (for the signal) was also used. Finally, the thrust value complemented this sample of discriminant variables.

5.4 Neural network

Three different neural networks have been trained for each year of data taking. The training of the network was performed with 100 epochs. After this step, the network was applied on the data, on the different backgrounds and on the signal. A step by step cut was performed on the network output. As an example, the result is presented in figure 3

in the muon channel for the 2000 year. For all the results, the agreement between data and simulation was globally correct, and no excess was observed.

Finally, no signal events were reported in the semi-leptonic channel in the data from 189 GeV to 209 GeV. This conclusion gave an exclusion on the signal. To improve the exclusion power, the working points were determined with the method already explained.

5.5 Results

The choice of the working points led to the results presented in table 4. A good agreement was observed for all the channels and for all energies. The total efficiencies are shown in table 5.

It was checked during the analysis that very few inversions between the b jet and the c jet occurred: the value of the *"b-tag"* of the c jet does not help for the signal discrimination. Consequently, this results applied without change to the process $e^+e^- \longrightarrow t\bar{u}$.

Electron	Data	Standard processes	4 fermions	$q\bar{q}$	$\gamma\gamma$
1998	2	2.3 ± 0.29	1.7	0.6	0.0
1999	4	3.1 ± 0.30	2.0	0.8	0.3
2000	6	11.6 ± 1.13	9.1	1.3	1.2

Muon	Data	Standard processes	4 fermions	$q\bar{q}$	$\gamma\gamma$
1998	1	1.1 ± 0.10	0.8	0.3	0.0
1999	3	2.5 ± 0.15	2.1	0.4	0.0
2000	5	5.3 ± 0.16	4.5	0.8	0.0

Tau	Data	Standard processes	4 fermions	$q\bar{q}$	$\gamma\gamma$
1998	4	3.7 ± 0.27	2.3	1.4	0.0
1999	10	8.3 ± 0.42	5.2	2.4	0.7
2000	9	10.7 ± 0.22	8.5	2.2	0.0

Table 4: Number of selected events after the final cut for the data and for the different standard processes (electron, muon and tau channel). The results are shown for the years 1998 to 2000. The quoted errors are only statistical.

Efficiency (%)	Electron	Muon	Tau	Total
1998	5.2 ± 0.49	5.5 ± 0.51	3.7 ± 0.42	14.4 ± 0.82
1999	3.2 ± 0.39	4.1 ± 0.44	3.6 ± 0.41	10.4 ± 0.70
2000	3.5 ± 0.41	4.6 ± 0.47	3.6 ± 0.42	11.7 ± 0.75

Table 5: Efficiencies for the signal after the final cut for each channel. The last column represents the efficiency for the three cumulated semi-leptonic channels.
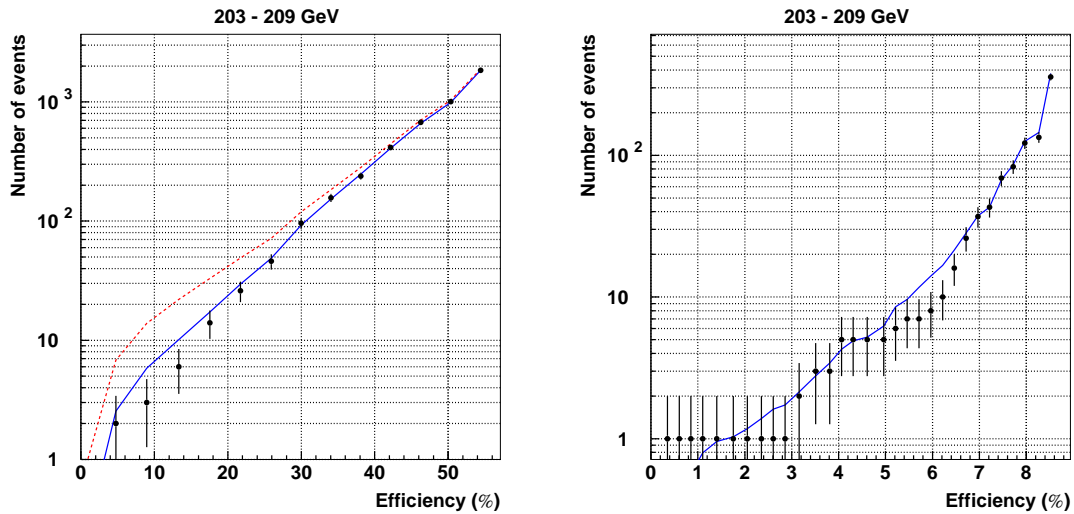
Figure 3: Number of selected events for the data collected at 203-209 GeV (dots) and for the total background (full line) versus total signal efficiency. Left plot: hadronic channel (the dashed line illustrates what would be expected for a signal with a cross-section equal to 0.4 pb). Right plot: muon channel.

6   Exclusion

6.1   Limit on the production cross-section

The study of the three years of data taking in the hadronic and the semi-leptonic channels showed that no signal $e^+e^- \longrightarrow t\bar{c}/t\bar{u}$ was observed. These results allowed to set a limit on the production cross-section of these signals. For each year, we combined the results obtained in the hadronic channel, in the electron, the muon and the tau channels (as they are strictly independent). The different collision energies have been also combined, which represents a total integrated luminosity of 608 pb^{-1}.

The combination has been performed thanks to the ALRMC software [20]. The combination between channels at the same energy does not require a model for the signal production. Therefore, the limits obtained in this case are independent of hypotheses on the production cross-section of $e^+e^- \longrightarrow t\bar{c}/t\bar{u}$. On the contrary, to combine samples at different energies requires the knowledge of the cross-section evolution (see equation 1). We chose to present the combined limits on the cross-section at an energy of 206 GeV (but the choice of 189 GeV or 200 GeV would be also appropriate). The results are presented in table 6. All limits were set with a confidence level of 95%. The statistical errors on the number of background events and on the signal efficiencies were taken into account in the computation.

The study of the table shows that the limits are similar for the three years of data taking. However, we notice worse results in the semi-leptonic channel for the data collected in 1999: it can be explained by the slight excess reported in table 4 for the three semi-leptonic channels.

The final result, for a collision at 206 GeV, is (at the 95% of confidence level):

$$\sigma(e^+e^- \longrightarrow t\bar{u} + \bar{t}u) \quad < \quad 0.11 \text{ pb};$$
$$\sigma(e^+e^- \longrightarrow t\bar{c} + \bar{t}c) \quad < \quad 0.11 \text{ pb}.$$

As it was shown previously, these results are valid when the mass of the exchanged squark is bigger than 70 GeV/c^2.

Sample	σ_H (pb)	σ_{SL} (pb)	σ_{H+SL} (pb)
1998 data (189 GeV)	0.25	0.26	0.16
1999 data (200 GeV)	0.22	0.43	0.19
2000 data (206 GeV)	0.23	0.29	0.16
Combination (206 GeV)	0.14	0.22	**0.11**

Table 6: Excluded cross-sections at the 95% of confidence level for the hadronic channel only (σ_H), for the semi-leptonic channel only (σ_{SL}) and for the combination of these two channels (σ_{H+SL}). The results are presented for the data collected in 1998, 1999 and 2000 (with, in brackets, the mean energy used for the computation of this limit). The last line gives the combined limit on the cross-section at an energy of 206 GeV (after combination of the three data samples).

6.2   Limit on the product of coupling constants

These limits can be translated into limits on the product of coupling constants involved in the interaction. The equation (2) of the production cross-section shows that it can be expressed as $\sigma = |\lambda'_{1jk}\lambda'^*_{13k}|^2 f(\sqrt{s}, m_{\widetilde{d}_k})$ with $j, k = \{1; 2\}$ and f a function of the collision energy and of the squark mass. Figure 4 presents the constraint obtained on the product of the coupling constants versus the squark mass. The uncertainty of ± 5.1 GeV/c^2 on the t quark mass was taken into account in this figure and corresponds to the band around the central curve.

For a squark mass of 100 GeV/c^2, the limit on the product of the coupling constants is equal to:

$$|\lambda'_{1jk}\lambda'^*_{13k}| < 0.043 \quad \text{(at the 95% of confidence level)}.$$

As anticipated, the limit obtained in this paper set less stringent constraints than those determined in a indirect way (see section 3). However, as it was already underlined, on the contrary to the previous studies, the searches presented here were based on a direct analysis of events with R-parity violation and permitted a probe of the λ' couplings.

7   Conclusion

For the first time, a signal $e^+e^- \longrightarrow t\bar{c}/t\bar{u}$ produced via λ' coupling constants have been searched for in a collider. The couplings are involved at the level of the particle production, giving the possibility to probe directly their values. In order to improve the sensitivity to these couplings, the two types of the W boson decay were studied.
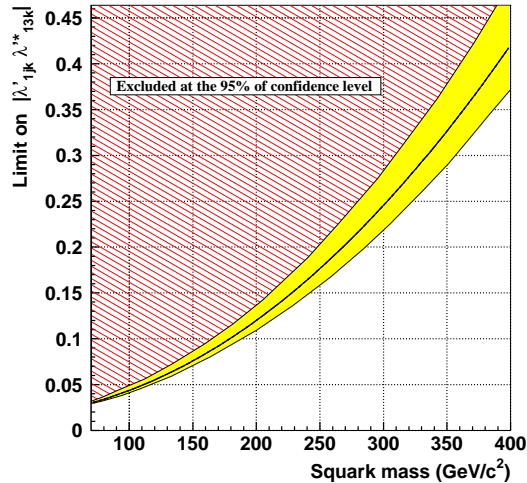
Figure 4: Limit on the product $|\lambda'_{1jk}\lambda'^{*}_{13k}|$ (with $j, k = \{1; 2\}$) versus the mass of the down-type squark. The central curve corresponds to the limit obtained for a t quark mass equal to 174.3 GeV/c^2 and the region around this curve takes into account the uncertainty of one standard deviation on the mass of this quark.

The analysis of the data from 1998, 1999 and 2000 (with a total integrated luminosity of 608 pb^{-1}) presented no significant excess. After combination of the different analyses, this result was interpreted in the framework of supersymmetry with R-parity violation, leading to the following limit on the production cross-section (at 206 GeV):

$$\sigma(e^+e^- \longrightarrow t\bar{u} + \bar{t}u) < 0.11 \text{ pb};$$
$$\sigma(e^+e^- \longrightarrow t\bar{c} + \bar{t}c) < 0.11 \text{ pb}.$$

These results are valid when the exchanged squark mass is bigger than 70 GeV/c^2 (lower masses were already excluded at LEP).

With the knowledge of the theoretical cross-section, these limits translate into constraints on the product of the coupling constants. For a down-type squark mass of 100 GeV/c^2, we obtained (for $j, k = \{1; 2\}$):

$$|\lambda'_{1jk}\lambda'^{*}_{13k}| < 0.043 \quad \text{(at the 95\% of confidence level)}.$$

8   Acknowledgements

References

[1] M. Drees, *An introduction to supersymmetry*, hep-ph/9611409.

[2] DELPHI collaboration, *Nucl. Instr. Meth.* **A303** (1991) 233;
DELPHI collaboration, *Nucl. Instr. Meth.* **A378** (1996) 57.

[3] U. Mahanta and A. Gosal, *R-parity violation contribution to $e^+e^-(\mu^+\mu^-) \longrightarrow t\bar{c}$*, hep-ph/9706398.

[4] M. Chemtob and G. Moreau, *Phys. Rev.* **D59** (1999) 116012, hep-ph/9806494.

[5] Y. Zeng-Hui *et al.*, *Probing R-parity violation in the production of $t\bar{c}(c\bar{t})$ on the lepton colliders*, hep-ph/9910323.

[6] S. Andringa *et al.*, *DELPHI note* 2001-087 CONF 515;
V. Obraztsov *et al.*, *DELPHI note* 2001-088 CONF 516.

[7] S. L. Glashow, J. Iliopoulos and L. Maiani, *Phys. Rev.* **D2** (1970) 1285.

[8] C-S. Huang *et al.*, *Phys. Lett.* **B452** (1999) 143.

[9] B. Mukhopadhyaya and A. Raychaudhuri, *Phys. Rev.* **D39** (1989) 280;
J. L. Lopez *et al.*, *New supersymmetric contributions to $t \longrightarrow cV$*, hep-ph/9702350.

[10] D. Atwood *et al.*, *Phys. Rev.* **D53** (1996) 1199.

[11] ALEPH collaboration, *Search for R-parity violating decays of supersymmetric particles in e^+e^- collisions at centre-of-mass energies from 189 GeV to 202 GeV*, hep-ex/0011008.

[12] Generator written by M. Besançon.

[13] DELPHI collaboration, *DELPHI note* 89-68 PROG 143.

[14] DELPHI collaboration, *DELPHI note* 89-44 PROG 137.

[15] H. Kroka, in *Proceedings of the 28th international conference on high energy physics*, July 1996.

[16] Y. Grossman *et al.*, *Nucl. Phys.* **B465** (1996) 369, hep-ph/9510378;
Y. Grossman *et al.*, *Nucl. Phys.* **B480** (1996) 753, hep-ph/9510378v3.

[17] Code implemented by A. Ouraou and L. Simard for the study of the W boson in DELPHI.

[18] Y. L. Dokshitzer *et al.*, *JHEP* **08** (1997) 001, hep-ph/9707323;
S. Bentvelsen, I. Meyer, *Eur. Phys. J.* **C4** (1998) 623.

[19] O. Couet, B. Mansoulié and J. Schwindling, MLPFIT,
`http://schwind.home.cern.ch/schwind/MLPfit.html`.

[20] A. L. Read, *DELPHI note* 97-158 PHYS 737.